First-principles theory of short-range order in size-mismatched metal alloys: Cu-Au, Cu-Ag, and Ni-Au

C. Wolverton, V. Ozoliņš, and Alex Zunger
National Renewable Energy Laboratory, Golden, Colorado 80401
~Received 20 October 1997!

We describe a first-principles technique for calculating the short-range order ~SRO! in disordered alloys, even in the presence of large anharmonic atomic relaxations. The technique is applied to several alloys possessing large size mismatch: Cu-Au, Cu-Ag, Ni-Au, and Cu-Pd. We find the following: ~i! The calculated

ideal fcc lattice sites, $\mathbf{R}_i^0$. We show below that this choice can lead to qualitatively incorrect SRO patterns for the systems studied here. A more correct description of the energy is as a function of ''relaxed'' equilibrium atomic positions $\mathbf{R}_i^{eq}$, determined by zero-force conditions for all $i = 1, \ldots, N$ atoms

$$\mathbf{F}_i = \frac{\partial E}{\partial \mathbf{R}_i} = 0. \tag{5}$$

Equations (3) and (4) demonstrate that the SRO is determined by a sampling of all configurations with a probabilistic weighting factor. The problem of predicting the equilibrium SRO pattern for a given alloy at x and T is then to evaluate Eqs. (3) and (4) which requires knowledge of $E(s, \mathbf{R}_i^{eq})$ for each s. It is important to notice that we use the *total* relaxed electron + ion energy $E(s, R_i^{eq})$ of configuration s. It thus contains (a) the sum of all occupied energy bands, (b) electron-electron Coulomb, exchange, and correlation, and (c) ion-ion terms. In contrast, the popular Fermi surface nesting construct[9] is often used to explain the SRO of Eqs. (1)–(4) by focusing instead on a single total energy term from the sum in (a) alone (the highest occupied band).

Theory and measurements of SRO in alloys formed from metal constituents with large size mismatch are challenging due to the fact that atoms ''relax'' away from their ideal lattice sites and move to energy-lowering positions given by Eq. (5). Even though local atomic relaxation does not alter the *identity* of atoms on given lattice sites (and hence, does not alter $\hat{S}_i$ or s in general), it does affect the energy $E(s, \mathbf{R}_i^{eq})$, and hence via Eqs. (3)–(5) will affect the propensity of developing a paticular type of SRO pattern in the alloy. These sometimes large atomic relaxations lead to difficulties in SRO treatments: Theoretically, the size mismatch requires one to treat the energetic effects of large atomic relaxations in all configurations, specifically, both random and partially ordered states (Eq. (3)). Experimentally, in diffuse scattering measurements, the atomic displacements themselves lead to diffuse scattering, complicating the separation of the portion of diffuse scattering due to SRO. Our calculations include the implicit effect of atomic displacements on $P(s, T)$ and therefore on the SRO contribution to diffuse scattering. However, we are not attempting to calculate the explicit contribution of atomic displacements to the diffuse scattering. A first-principles total-energy method capable of treating not only the chemical effects of SRO but

thermodynamics is to perform statistical calculations by

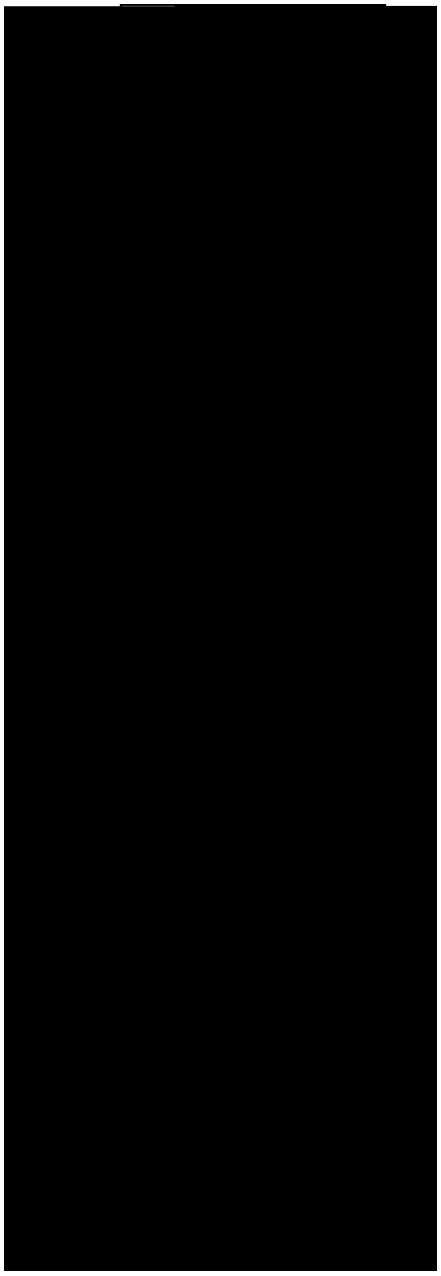

FIG. 1. The calculated constituent strain energies for Cu-Au, Cu-Ag, and Ni-Au along several principle directions.

Here, we use mixed-space CE Hamiltonians that have been constructed using fully relaxed, full-potential, linearized augmented plane-wave, total energies for the fcc-based Cu-Au, Cu-Ag, and Ni-Au systems. For each alloy, the mixed-space CE has been fit to total energies of ; 30–35 ordered compounds and epitaxial energies for ; 5–6 different orientations ~see Ref. 36 for details of the LDA calculations and CE construction for these systems!.

C. Monte Carlo details

In order to discern the equilibrium SRO in the alloys of interest here, we have subjected the mixed-space CE of Eq. ~6! to Monte Carlo simulations in the canonical ~fixed composition! ensemble.[42] We have used fcc unit cells with sizes of 24^3–32^3 5 13824–32768 atoms. $a_{lmn}(x)$ are computed by taking thermal averages of the spin products ^ P $_{lmn}$& and then using Eq. ~1! to obtain the SRO parameters. Using a finite number n_R of these real-space shells in Eq. ~2!, we obtain the SRO in reciprocal space, $a(x,\mathbf{k})$. Tests have been performed to ascertain the number of Monte Carlo steps required for convergence of the SRO. We have used . 1000 Monte Carlo stops ~MCS! for taking averages of the SRO; this is preceded by ; 100–500 MCS for equilibration. For SRO in the disordered phase, the Monte Carlo algorithm converges quite quickly; thus, large cell sizes and large number of MCS were only necessary in cases of determining very subtle features of the SRO pattern ~e.g., the temperature dependence of the fourfold SRO splitting in Cu-Au or Cu-Pd!. We have calculated the SRO using several different random number generators in the Monte Carlo algorithm. Only very subtle features such as SRO splitting were affected in any significant way. We settled on the generator from the ESSL libraries.[43]

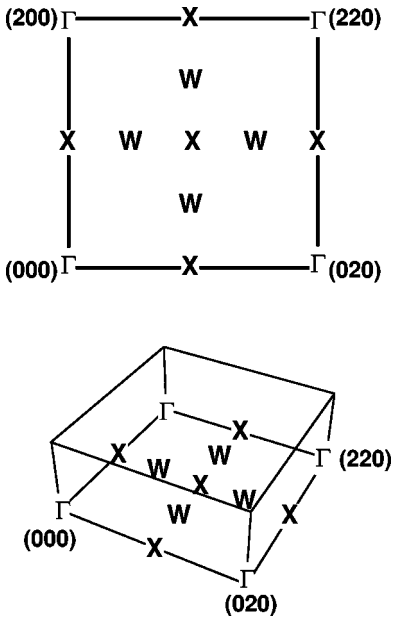

FIG. 2. Schematic plot of ($hk0$) plane of reciprocal space, with high-symmetry points labeled. The plane is shown from the perspectives used in both the contour and three-dimensional plots in this paper.

For all of the alloys studied here, the ($hk0$) plane in reciprocal space @which contains the high-symmetry G(5 ^000&), X(5 ^100&), and W(5 ^1 $\frac{1}{2}$ 0&) points# contains the SRO peak positions. Therefore, for all SRO plots in reciprocal space, we show only the ($hk0$) plane. A schematic plot of this plane of reciprocal space is shown in Fig. 2 along with the high-symmetry points.

III. CONSTITUENT STRAIN: RELEVANCE TO SRO

Here we discuss the constituent strain energies @Eq. ~7!# for the alloy systems of interest ~Cu-Au, Cu-Ag, and Ni-Au! and give some indications of the conditions under which this strain energy is expected to play a major role in determining the SRO. The constituent strain energies for Cu-Au, Cu-Ag, and Ni-Au are shown in Fig. 1 for several principle directions. The strain energies for these three systems look quali-

tatively similar, with each alloy showing the same crossover of the minimal strain energy with composition: The ^100& strain is minimal for alloys where the ''large atom'' ~Au or Ag! is in the majority ~e.g., Au-rich Cu-Au, Au-rich Ni-Au, or Ag-rich Cu-Ag!. However, for alloys where the ''small atom'' ~Cu or Ni! is in the majority ~e.g., Cu-rich Cu-Au, Ni-rich Ni-Au, or Cu-rich Cu-Ag!, the ^201& direction becomes the elastically softest direction. This crossover of soft strain direction is forbidden in harmonic elasticity theories, and hence is due to anharmonic strain effects.[41]

The energetic effects of constituent strain are expected to be particularly relevant for determining SRO in alloys whose energetics are dominated by strain. In particular, phase-separating alloys are most likely to exhibit ''clustered'' *A*-rich or *B*-rich regions. The strain energy required to maintain coherency between these *A*-rich and *B*-rich regions is physically related to the constituent strain energy. Thus, we expect the constituent strain to be most relevant for deciding the SRO tendencies in phase-separating alloys ~Cu-Ag and Ni-Au!, and less so in ordering alloys ~Cu-Au!. As we show below, we indeed see manifestations of the crossover of the elastically soft direction on the SRO of Cu-Ag and Ni-Au alloys, but not in Cu-Au.

Equation ~6! shows that the alloy Hamiltonian used in the Monte Carlo simulations is composed of three parts: the pair interaction terms, the multibody interaction terms, and the constituent strain terms. We show below calculations of SRO using all three parts of the Hamiltonian. However, given the discussion of the relevance of constituent strain to SRO, it is interesting to see the SRO pattern produced by considering the constituent strain *only*. Thus, in addition to the ''full'' calculations, which contain pairs, multibodies, and constituent strain in the alloy Hamiltonian, we have also computed the SRO with the CS energy only. These results are shown in Fig. 3, where we have used the $Ni_{0.4}Au_{0.6}$ and $Ni_{0.1}Au_{0.9}$ alloys as examples. From Fig. 1 it is clear that the constituent strain energy is very similar for the three alloy systems, so we do not expect the ''strain-only'' results for Ni-Au to be qualitatively different from Cu-Au or Cu-Ag at analogous compositions. ~Because the CS energy is nonanalytic in reciprocal space about the origin, many Fourier coefficients are

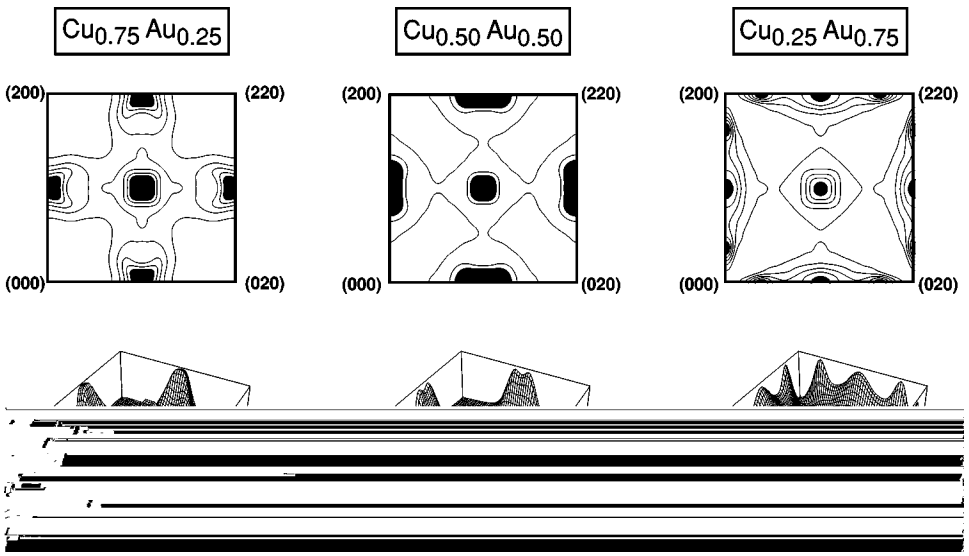

FIG. 4. The calculated SRO patterns in $Cu_{0.75}Au_{0.25}$, $Cu_{0.5}Au$

~i! $Cu_{0.75}Au_{0.25}$: The LRO of Cu_3Au is of $L1_2$ type, characterized by ^100& composition waves. The SRO of $Cu_{0.75}Au_{0.25}$ shows a very slight fourfold splitting of the calculated SRO peaks off of the X point along the ^1*z*0& direction. This fourfold splitting has been measured, and these measurements will be compared with the calculated splitting and will be discussed in detail in Secs. IV B and IV C. The comparison of calculated real-space Warren-Cowley SRO parameters a_{lmn} @Eq. ~1!# with those from several experimental measurements for $Cu_{0.75}Au_{0.25}$ are given in Table I, showing good agreement with the measured values ~note that of the experimental data cited, Ref. 18 is probably the most modern, at-temperature measurement!: Almost all values fall well within the spread between different experimental values. The first- ~second-! neighbor parameters are predicted to be the dominant parameters, having strong ordering ~clustering! tendencies, in agreement with all the measured values. After the first and second neighbors, the next largest parameter is calculated to be for the fourth-neighbor shell, with another cluster tendency. Again, this aspect of the calculation agrees with the measured values. @Note that the reciprocal-space SRO pattern of $Cu_{0.75}Au_{0.25}$ is clearly of ordering type, even though two of the three largest real-space SRO parameters ~second- and fourth-neighbor! are positive, indicating clustering in these shells. Thus, it it easier to determine the overall clustering/ordering tendency by examining the pattern in reciprocal space, rather than by examining individual a_{lmn} in real space.# The biggest discrepancy between calculated and measured values is in the third-neighbor shell. The calculations give a negative ~ordering!

value of $a_{211} = -0.027$, one measurement[7] gives a slightly weaker ordering value of $a_{211} = -0.012$, but all the other measured values give clustering values $a_{211} > 0$. It is interesting to note that the one measurement that gives $a_{211} < 0$ was performed for alloys quenched from two different temperatures and found the value of this parameter to be quite sensitive to temperature, with a_{211} getting more negative with decreasing temperature. The calculations were performed at a temperature ($T = 650$ K) 38–73 K lower than the measured values.

$Cu_{0.5}Au_{0.5}$: The calculated SRO of $Cu_{0.5}Au_{0.5}$ shows a very small splitting, but at this composition, the calculated splitting is twofold along the $\langle z00 \rangle$ direction. A comparison of calculated and measured real-space SRO parameters for various compositions $Cu_{1-x}Au_x$ is given in Table II. For the sake of space, we have only listed one set of measured SRO parameters for each composition

to SRO is not precisely at the X point, but rather that there is a fourfold splitting of this peak in the $\langle 1z0 \rangle$ direction. Reichert, Moss, and Liang[31] have recently measured the temperature dependence of this splitting *in situ* and have observed, interestingly, an increase in splitting with increasing temperature. Using our theoretical approach, we have thus examined the fine structure of the SRO peaks in $Cu_{0.75}Au_{0.25}$ as a function of temperature in an effort to ascertain the origin of ~1! the fourfold splitting itself, and ~2! the temperature-dependence of said splitting. Another alloy for which X-point fourfold splitting has been observed[10] is $Cu_{0.70}Pd_{0.30}$. First-principles calculations[56,57,38] have reproduced this peak splitting in $Cu_{0.70}Pd_{0.30}$ at fixed temperature. Additionally, near Cu_3Pd stoichiometry, long-period superstructures are observed at low temperatures, in contrast to the situation for Cu_3Au where $L1_2$ is the low-temperature stoichiometric ground state. This makes Cu_3Pd a potentially interesting contrast to Cu_3Au. Because a mixed-space CE for Cu-Pd has already been constructed using LDA energetics,[57] we use this Hamiltonian to examine the fine structure and temperature dependence of the SRO peaks in $Cu_{0.70}Pd_{0.30}$ so as to provide a comparison with the case of $Cu_{0.75}Au_{0.25}$.[58]

Figure 5 shows the calculated SRO intensity in disordered $Cu_{0.70}Pd_{0.30}$ and $Cu_{0.75}Au_{0.25}$ alloys along the $\langle 1z0 \rangle$ line in reciprocal space. Both $Cu_{0.70}Pd_{0.30}$ and $Cu_{0.75}Au_{0.25}$ alloys show a splitting of the SRO peak off the X point, in agreement with measurements. The splitting is quantified by z, the distance ~in units of $2p/a$) of the SRO peak from the X point. The calculated low-T splitting wave vectors in $Cu_{0.70}Pd_{0.30}$ $z = 0.13(2p/a)$ and in $Cu_{0.75}Au_{0.25}$ $z = 0.05(2p/a)$ are in excellent agreement with the measured values of $z = 0.13 \pm 0.14$ ~Refs. 59 and 10! and $z = 0.05$,[31] respectively.[60]

We wish to determine the thermodynamic origin of ~1! the *existence* of SRO splitting in these alloys and ~2! the *temperature dependence* of such splitting. First, we examine the origin of the *existence* of the splitting. We find that the qualitative differences in the total energies of $Cu_{0.75}Au_{0.25}$ and $Cu_{0.70}Pd_{0.30}$ lead to the conclusion that the SRO splitting in $Cu_{0.75}Au_{0.25}$ cannot be inferred from $T = 0$ K energies alone. However, the splitting in $Cu_{0.70}Pd_{0.30}$ can be inferred from $T = 0$ K energies alone: Figure 6 depicts the cluster-expanded $T = 0$ K structural energies $\Delta E(z) = (1/2m)\# = E(1/2m)\# - 2E(0)$ of $L1_2$ ''long-period superstructures'' ~LPS's!. One subset of these LPS's are formed from $L1_2$ ($m = \infty$) by inserting an antiphase boundary every m cells and have ''fundamental'' superstructure peaks at $(1z0)$ where $z = 1/2m$. ~There are, in general, other ''harmonic'' wave vectors corresponding to lower amplitude composition waves used to build the LPS. For example, see Refs. 61 or 62.! In Cu_3Pd, a structure with an intermediate (m_0 ; 3 2 4 or z ; 0.17 2 0.12) value is predicted to be more stable than $L1_2$ ($z = 0$) at $T = 0$ K. This implies that there is an *energetic* lowering for fluctuations in the disordered $Cu_{0.70}Pd_{0.30}$ alloy of the z ; 0.17 2 0.12 type that produce splitting in the SRO peaks. For Cu_3Au LPS, however, we find that $\Delta E(1/2m) > 0$ at $T = 0$ K for all m and therefore these LPS are not ground-state structures, in qualitative contrast with Cu_3Pd. This means that *there is no energetic gain for fluctuations that produce SRO splitting in* $Cu_{0.75}Au_{0.25}$. The fact that the splitting exists nonetheless in our calculations ~even though there is an energetic penalty for such splitting! clearly demonstrates that the existence of the calculated SRO splitting in Cu_3Au is due to entropic effects. Further, because the only entropic effect we have included in our calculations is configurational, one can conclude that *configurational entropy is necessary to account for the SRO splitting in* $Cu_{0.75}Au_{0.25}$.

Another way to see the distinction between the energetics of $Cu_{0.75}Pd_{0.25}$ and $Cu_{0.75}Au_{0.25}$ is to examine the Fourier transform $J_{\text{total}}(\mathbf{k})$ of the Hamiltonian used to generate the SRO patterns in Fig. 5. Figure 7 shows the calculated $J_{\text{total}}(\mathbf{k})$ for $Cu_{0.75}Pd_{0.25}$ and $Cu_{0.75}Au_{0.25}$ along the $\langle 1z0 \rangle$ line in reciprocal space. In these figures, we have included all contributions of the mixed-space CE Hamiltonian of Eq. ~6!:

$$J_{\text{total}}(\mathbf{k}) = J_{\text{pair}}(\mathbf{k})$$

where the three terms are the pair interactions, the multibody interactions, and the constituent strain.[63] The minimum in $J_{\text{total}}(\mathbf{k})$ for $Cu_{0.75}Au_{0.25}$, which demonstrates the lowest *energy* point along this line, does not occur for some intermediate $z \neq 0$, but rather occurs *at* the X point. Thus, as stated before, the internal energy alone for this Hamiltonian will not produce SRO fluctuations with a fourfold splitting ~since there is an energetic penalty for $z \neq 0$ fluctuations!. Since our $T \neq 0$ Monte Carlo results using the energetics shown in Fig. 7 nonetheless produce a SRO splitting, we conclude that it is the configurational entropy that moves the minimum in free energy towards some $z \neq 0$ position and hence produces a splitting the SRO peaks.

In qualitative contrast to $Cu_{0.75}Au_{0.25}$, $J_{\text{total}}(\mathbf{k})$ for $Cu_{0.75}Pd_{0.25}$ shows a minimum for an intermediate wave vector between the X and W points ($z \sim 0.14$). This means that fluctuations with wave vectors $\langle 1z0 \rangle$ ($z \sim 0.14$) will be energetically favorable, and thus the thermodynamic origin of the SRO splitting in $Cu_{0.75}Pd_{0.25}$ is energetic rather than entropic.

The duality noted in the Introduction between commensurate LRO and incommensurate SRO in Cu_3Au is analogous to what is expected from the 2D ANNNI model[65]: In this model, if the ratio between the second- and first-neighbor

the prediction of splittings for compositions other than $Cu_{0.75}Au_{0.25}$

doing so poses no difficulty in principle if one were interested in determining the existence ~or absence! of SRO splitting in CuAu or $CuAu_3$.

V. SHORT-RANGE ORDER IN $Cu_{1-x}Ag_x$

$Cu_{1-x}Ag_x$ is quite distinct from $Cu_{1-x}Au_x$ in its low-temperature phase stability. While $Cu_{1-x}Au_x$ forms ordered compounds which disorder and lead to a complete solubility of the solid solution at high temperatures, $Cu_{1-x}Ag_x$ phase separates at all temperatures up to the melting points of both Cu and Ag. There is only limited solubility of Cu in Ag @ ; 14% at T 5 1050 K ~Ref. 51!# and of Ag in Cu @ ; 5% at T 5 1050 K ~Ref. 51!#. Also, different from $Cu_{1-x}Au_x$ where a large number of measurements of SRO exist, to the authors' knowledge, no SRO measurements exist for

is for the second-neighbor shell, which has a strong clustering-type tendency. Most of the calculated SRO parameters have the same sign as the measured ones, with two notable exceptions: The nearest-neighbor SRO parameter is small and negative in our calculations ~indicating a slight ordering tendency in the nearest-neighbor shell!, while Wu and Cohen find a small positive ~clustering! value. The other discrepancy between calculation and experiment occurs in the ~400! shell. It is interesting, however, that the nearest-neighbor and ~400! shells are the only ones for which the experimental error ~shown in parentheses in Table IV! is larger than the measured value itself, and thus, the sign of these parameters is in some doubt. We also show in Table IV that earlier x-ray measurements on polycrystalline samples[4] show a nearest-neighbor SRO parameter that is negative.

Warren-Cowley SRO parameter; and ~2! noted, in a simulation based on the measured SRO parameters, clusters of Ni atoms, with the wavelength of these clusters corresponding to the peak of the measured SRO pattern in reciprocal space, $\mathbf{k}_{\mathrm{SRO}}$; (0.6,0,0). These facts indicate a short-range *clustering* tendency along the ~100! direction. Our calculations agree with these observations. However, there is a semantic problem of how to characterize these facts when considering all of the measured data. We characterize the measured and calculated SRO pattern as *ordering type* since: ~1! The total SRO pattern in reciprocal space ~including 25 real-space shells! shows peaks *away* from the G point, the latter being the typical wave vector for clustering-type tendencies. As we saw in Cu-Au, the gross ordering/clustering tendency is easier to determine by examining the SRO pattern in reciprocal space rather than looking at individual real-space shells. ~2! The Warren-Cowley SRO parameters in real space show strong negative ~ordering-type! values in many shells *other* than second neighbor, indicating that the clustering tendency in the second shell is competing with an ordering tendency in many other shells.

Several authors have tried to account for the rather surprising result that even though Ni-Au is a phase-separating alloy, the measured peak intensity in reciprocal space due to SRO is of ordering type and occurs at the point $\mathbf{k}_{\mathrm{SRO}}$; (0.6,0,0), rather than $\mathbf{k}_{\mathrm{SRO}}$ 5 (0,0,0) which would be expected for a clustering alloy. Lu and Zunger[40] calculated the SRO ~using 21 real-space shells! and found peaks at ; (0.8,0,0) whereas Asta and Foiles[73] used an embedded

Thus, this is the formation energy of a structure whose volume is hydrostatically deformed to equilibrium, but all cell-internal and cell-external positions are ideal.

Ordered, Relaxed: $\Delta E_{\mathrm{VD}} + dE_{\mathrm{UR}}^{\mathrm{chem}} + dE^{\mathrm{int}} + dE^{\mathrm{ext}}$. The relaxed energies include all four terms in ΔH. Thus, the difference between unrelaxed and relaxed energies is simply the last two terms, $dE^{\mathrm{int}} + dE^{\mathrm{ext}}$, the energy gained upon cell-internal and cell-external distortions of the unit cell from their ideal values.

We are interested in SRO in disordered alloys, which is a phenomenon probing *coherent* configurations of atoms, and thus for the interpretations of this section, we must define geometries and energetics that correspond to unrelaxed and relaxed energies of ''coherent ordered'' and ''coherent phase-separated'' states. Because SRO probes the properties of coherent configurations, the energetics of incoherent configurations ~such as ''$A + B$'' where A and B are each at their equilibrium lattice constants!

are not effected by our specific choice of ordered compound.! Thus, one would expect that an ordering-type SRO would result for each of the three alloys, constrained to unrelaxed geometries. Calculations using unrelaxed LDA energetics bear out this expectation: Using a technique analogous to that described in Sec. II, we have fit the *unrelaxed* LDA energies of a large number of Cu-Ag compounds to a cluster expansion Hamiltonian. Subsequent Monte Carlo calculation using this Hamiltonian yields a SRO pattern ~not shown here! for ''unrelaxed Cu-Ag'' which is ordering type, with peaks at the X point. Similar X-point ordering-type SRO patterns have been predicted for unrelaxed Cu-Au ~Ref. 49! and Ni-Au.[73] Thus, ~i! in Cu-Au, the X-point peaks are not qualitatively affected by relaxation, while ~ii! in Ni-Au, relaxation moves the SRO peak from the X point toward the origin of reciprocal space to a point along the $\Gamma 2X$ line. ~iii! In Cu-Ag, relaxation moves the SRO peak from an ordering-type positions (X point! to a clustering type position ~near the Γ point!, reversing the *qualitative ordering tendencies* of the disordered alloy. These predictions are in accord with the proof of Asta and Foiles,[73] who showed that under certain restrictions, relaxation can only move an ordering-type SRO peak towards the Γ point.

VIII. SUMMARY

In this paper, we have described a first-principles technique for calculating the short-range order ~SRO! in disordered alloys, even for alloys with large size mismatch, where harmonic elastic theories are invalid. The technique has been applied to several alloys possessing large lattice mismatch: Cu-Au, Cu-Ag, and Ni-Au. We have demonstrated that the anharmonic strain energetics are most important and can produce qualitatively new effects in the SRO of phase-separating alloys.

Cu-Au alloys. We have found SRO peaks at ~or near! the $\{100\}$ point for all compositions studied ($x_{\mathrm{Au}} = 0.25,\ 0.50,$

[1] M. A. Krivoglaz, *Diffuse Scattering of X-rays and Neutrons by Fluctuations* ~Springer, New York, 1996!.
[2] L. H. Schwartz and J. B. Cohen, *Diffraction from Materials* ~Academic Press, New York, 1977!.
[3] J. M. Cowley, J. Appl. Phys. **21**, 24 ~1950!.
[4] P. A. Flinn, B. L. Averbach, and M. Cohen, Acta Metall. **1**, 664 ~1953!.
[5] B. W. Roberts, Acta Metall. **2**, 597 ~1954!.
[6] B. W. Batterman, J. Appl. Phys. **28**, 556 ~1957!.
[7] S. C. Moss, J. Appl. Phys. **35**, 3547 ~1964!.

[62] G. Ceder, D. de Fontaine, H. Dreysse, D. M. Nicolson, G. M. Stocks, and B. L. Gyorffy, Acta Metall. Mater. **38**, 2299 ~1990!.
[63] Because no long-range multibody interactions were included in the CE, these interactions cannot stabilize any LPS other than $L1_2$ or $D0_{22}$